

# Linear Stability Analysis of Solitons Governed by the 2D Complex Cubic-Quintic Ginzburg-Landau Equation

Emily Gottry <sup>†</sup>

*Faculty advisor: Edwin Ding, Ph.D.*

---

**Abstract.** We used the singular value decomposition to construct a low-dimensional model that qualitatively describes the behavior and dynamics of optical solitons governed by the complex cubic-quintic Ginzburg-Landau equation in two spatial dimensions. With this model, it was found that a single soliton destabilizes and transitions into a double-soliton configuration through an intermediate periodic phase as the gain increases. Linear stability analysis then revealed that a Hopf bifurcation occurs at several critical gain values corresponding to the destabilization of the single and double solitons.

**1. Introduction.** The study of nonlinear waves originated in 1834 when John Scott Russell, a Scottish engineer, was conducting experiments to determine the optimal design for canal boats [1]. One of the major results was his discovery of, in his own words, the *great wave of translation*, or *solitary wave*, as it is known today. Russell's discovery subsequently motivated the mathematical study of water waves by Stokes [2], Boussinesq [3], and Korteweg and de Vries [4], but it was not until 1965 when Zabusky and Kruskal made the breakthrough discovery of *solitons*, i.e., solitary waves that demonstrate particle-like behaviors, which led to extensive theoretical formulations and numerical simulations of nonlinear waves [5, 6]. Today, the study of solitons is of broad scientific interest. It pertains to the understanding of water wave propagation in the ocean, atmospheric turbulence, optical fiber transmission, and light-matter interaction, to name a few.

In the field of laser optics, the *master mode-locking equation* proposed by Haus in 1975 [7] is the most influential and fundamental governing equation. It is a nonlinear Schrödinger equation-based model that describes the formation and dynamics of optical solitons in 1-dimensional laser systems. In this project, we studied the time evolution of optical solitons in a 2-dimensional laser cavity governed by the complex cubic-quintic Ginzburg-Landau equation (CQGLE) [8]. The CQGLE generalizes Haus' model to give a more accurate description of the dominant physical effects in the laser cavity. Compared to Haus' model, the CQGLE includes a quintic correction term for the self-phase modulation and saturable absorption (intensity discrimination), as well as a bandwidth-limited saturated gain instead of a constant gain. Ginzburg-Landau equations are of significant physical importance as they arise in a variety of nonlinear wave and pattern-forming systems [9, 10].

In two spatial dimensions, with normalized parameters, the CQGLE is the partial differential equation (PDE) given by

$$(1.1) \quad i \frac{\partial u}{\partial t} + \frac{D}{2} \nabla^2 u + (\gamma - i\beta)|u|^2 u - (\nu - i\mu)|u|^4 u = ig(t)(1 + \tau \nabla^2)u - i\delta u ,$$

---

<sup>†</sup>Department of Mathematics, Physics, & Statistics, Azusa Pacific University, Azusa, CA 91702 (egottry18@apu.edu).

where

$$(1.2) \quad g(t) = \frac{2g_0}{1 + \|u\|^2/e_0}.$$

The complex variable  $u$  defines the amplitude of the electromagnetic field as a function of the spatial variables  $x$  and  $y$  and time  $t$ , and the Laplacian operator  $\nabla^2$  is taken with respect to the spatial variables.  $D$  is the averaged diffraction coefficient, and  $\gamma$  and  $\nu$  represent the cubic and quintic self-phase modulations, respectively. The cubic gain term  $|u|^2u$  with positive constant  $\beta$  models the pulse-forming mechanism in the laser cavity that preferentially amplifies the high-intensity portion of the electromagnetic field and attenuates the low-intensity portion to form a soliton, while the quintic loss (the term with coefficient  $\mu$ ) saturates the cubic gain and thus prevents the amplitude of the soliton from blowing up. The terms on the right side of the CQGLE represent other dissipative effects in the laser cavity. The gain function  $g(t)$ , which is saturated by the total cavity energy  $\|u\|^2 = \int_{-\infty}^{\infty} \int_{-\infty}^{\infty} |u|^2 dx dy$ , is controlled by the parameters  $g_0$  (pumping strength) and  $e_0$  (saturated pulse energy). The parameter  $\tau$  measures the bandwidth of the gain, and  $\delta$  is the total linear loss.

The goal of this research was to study the impact of the gain on the stability and shape of optical solitons governed by the CQGLE, so we first solved the PDE numerically in MATLAB using a spectral discretization in  $x$  and  $y$  and a Runge-Kutta time-stepping algorithm in  $t$ . We adjusted the pumping strength  $g_0$  while holding all other system parameters fixed. Unless stated otherwise, the parameters are assumed to be  $D = 0.5$ ,  $\gamma = 1.5$ ,  $\beta = 0.8$ ,  $\mu = 0.5$ ,  $\nu = 0.08$ ,  $e_0 = 1$ ,  $\tau = 0.1$ , and  $\delta = 1$ . A localized white noise was used as the initial condition for the CQGLE.

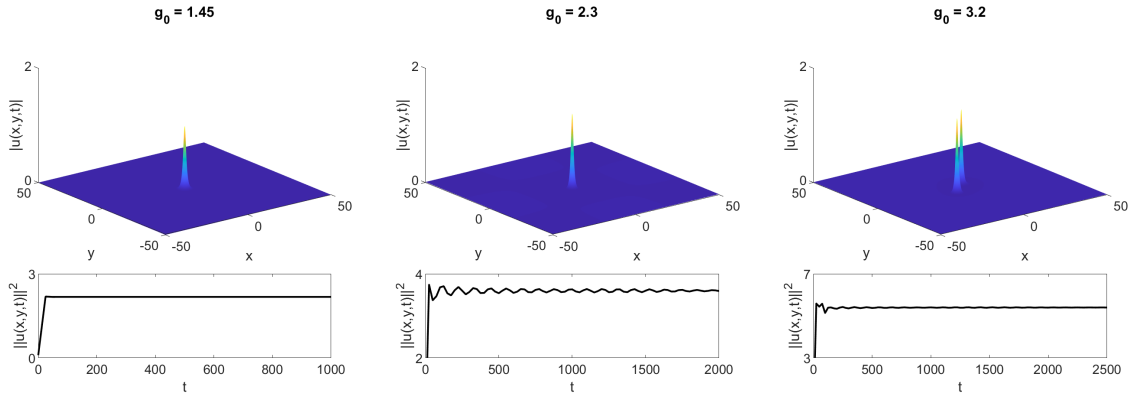


**Figure 1.** Top: Snapshots of stable single soliton, pulsating soliton, and stable double soliton of the CQGLE at different  $g_0$  values. Bottom: The corresponding time evolution of the total cavity energy  $\|u\|^2$ .

The top panels in [Figure 1](#) show snapshots of the numerical solution of the CQGLE at various  $g_0$  values, while the bottom panels plot corresponding time evolutions of the total cavity energy  $\|u\|^2$ . At a moderate pumping strength of  $g_0 = 1.45$ , the white noise initial condition self-organizes into a single soliton that remains stable throughout the rest of the simulation. When  $g_0$  is increased to 2.3, the amplitude and width of the soliton fluctuate

slightly over time, which causes periodic fluctuations in its energy as seen in the corresponding graph. At a high  $g_0$  value such as 3.2, these periodic oscillations are no longer observed, and the system settles onto a double-pulse configuration known as a double soliton. The two pulses in this case are identical to each other and have a greater amplitude than the single soliton.

Performing full numerical simulations on the CQGLE is time-consuming. Depending on the number of time steps and the size of the computational domain, each run takes up to a full week or longer to execute. This makes it extremely inefficient to study the transitions among different soliton states by direct simulation. Principal component analysis (PCA) is a popular technique in data analysis that aims to represent the maximum amount of information in a data set using only a small set of key features known as the principal components. In this work, we used PCA to derive a low-dimensional model to qualitatively reproduce each of the observations in [Figure 1](#). This model also supports a dynamical systems approach to analyze optical solitons governed by the CQGLE in two spatial dimensions. We aimed to efficiently characterize the transitions among the single-periodic-double soliton sequence as a function of the pumping strength  $g_0$  without running extensive full simulations.

The paper is organized as follows: The construction of the low-dimensional model is described in [section 2](#). Results based on numerical simulations of this model are presented in [section 3](#). Linear stability analysis of the low-dimensional model is discussed in [section 4](#), followed by conclusions from the results in [section 5](#).

**2. Low-Dimensional Model for the CQGLE.** Let  $\phi_1(x, y)$ ,  $\phi_2(x, y)$ , ... represent the principle components, or modes, of the soliton dynamics governed by the CQGLE. These are essentially the key soliton profiles observed in the evolution history of the electromagnetic field amplitude  $u(x, y, t)$ . Mathematically [[11](#), [12](#)], the  $n$ -th mode  $\phi_n(x, y)$  is the  $n$ -th eigenfunction that satisfies the eigenvalue problem

$$(2.1) \quad \int_{-\infty}^{\infty} \int_{-\infty}^{\infty} K(x, y, x', y') \phi_n(x', y') dx' dy' = \lambda_n \phi_n(x, y).$$

Here the non-negative constant  $\lambda_n$  is the eigenvalue associated with  $\phi_n(x, y)$ , and the kernel  $K(x, y, x', y')$  is the time-average of the product  $u(x, y, t) \overline{u(x', y', t)}$ , where the overbar denotes complex conjugation. In addition, the modes satisfy the orthonormality condition

$$(2.2) \quad \langle \phi_m, \phi_n \rangle = \int_{-\infty}^{\infty} \int_{-\infty}^{\infty} \phi_m \overline{\phi_n} dx dy = \begin{cases} 1, & m = n, \\ 0, & m \neq n. \end{cases}$$

Once the modes are found from [\(2.1\)](#), they can then be used to convert the CQGLE into a system of first-order ordinary differential equations (ODEs). The procedure is the same as solving linear PDEs using eigenfunction expansions. In particular, we expand  $u(x, y, t)$  in terms of the modes (eigenfunctions) as

$$(2.3) \quad \begin{aligned} u(x, y, t) &= \sum_{n=1} r_n(t) e^{i\theta_n(t)} \phi_n(x, y) \\ &= e^{i\theta_1(t)} \left( r_1(t) \phi_1(x, y) + \sum_{n=2} r_n(t) e^{i\psi_n(t)} \phi_n(x, y) \right), \end{aligned}$$

where the real-valued functions  $r_n(t)$  and  $\theta_n(t)$  represent the modal amplitude and phase associated with the  $n$ -th mode, respectively. The phase of the first mode is factored out so that  $\psi_n(t) = \theta_n(t) - \theta_1(t)$  measures the phase difference between the  $n$ -th mode and the first mode. Substituting this expansion into the CQGLE (1.1), applying the orthonormality condition (2.2), and separating the real and imaginary parts leads to the following system of first order, nonlinear ODEs:

$$(2.4) \quad \begin{cases} r'_n = F_n(r_1, \dots, \psi_2, \dots) & , \quad n = 1, 2, \dots \\ \psi'_n = G_n(r_1, \dots, \psi_2, \dots) & , \quad n = 2, 3, \dots \end{cases}$$

In the theory of PCA, the relative importance of the modes is ranked by the eigenvalues  $\lambda_1, \lambda_2$ , etc. Modes with greater eigenvalues are more dominant than the others and therefore capture more information about the data. Technically speaking, the above ODE system is an infinite dynamical system since there are infinitely many  $\phi_n$ 's. To arrive at a low-dimensional description of the CQGLE while retaining most of its important underlying dynamics, we truncate (2.3) to keep only the modes with the largest eigenvalues, which in turn gives us an ODE system with only a few equations.

The difficulty in carrying out the procedure described above is that the modes cannot be found in closed form since  $u(x, y, t)$  and hence the kernel function  $K$  in the eigenvalue problem (2.1) are not known a priori. We therefore take a numerical approach. First, we compute the numerical solution  $u(x, y, t)$  of the CQGLE at a particular  $g_0$  value, which is then stored in a matrix where each row corresponds to a particular time step. To account for both the single- and double-pulse shapes, we stack the data matrices of a single soliton simulation and a double soliton simulation vertically to form a combined data matrix  $A$ . In the numerical case, the modes  $\phi_1(x, y), \phi_2(x, y), \dots$  are approximated by orthogonal vectors  $\Phi_1, \Phi_2, \dots$  that satisfy the eigenvalue problem

$$(2.5) \quad A^* A \Phi_n = \lambda_n \Phi_n .$$

The asterisk denotes the conjugate transpose, so  $A^* A$  is the covariance matrix of the numerical data. Each eigenvector  $\Phi_n$  is normalized according to the orthonormality condition (2.2) where the integral is calculated numerically over the computational domain. It is well-known in linear algebra that the solution to the above matrix problem is equivalent to the singular value decomposition (SVD) of  $A$ ; the  $\Phi_n$ 's are given by the right singular vectors, and the  $\lambda_n$ 's are given by the square of the singular values.

Figure 2 shows the first four dominant modes in the combined data matrix  $A$ , along with their associated eigenvalues. As expected, the two most dominant soliton profiles in the numerical data matrix are in the shapes of a single soliton (top right panel) and double soliton (top left panel). The two following modes are combinations of shapes that are seen during the transient stage of the evolution. Experimentally, it was determined that the 11 most dominant modes were sufficient to qualitatively capture the essential dynamics of both the single and double solitons [13]. Using the eigenvalues, the percentage of information contained in the  $m$  most dominant modes can be calculated by dividing the sum of the  $m$  largest eigenvalues by the sum of all eigenvalues. Our 11 most dominant modes contain over 99.9% of the information from the two numerical simulations.

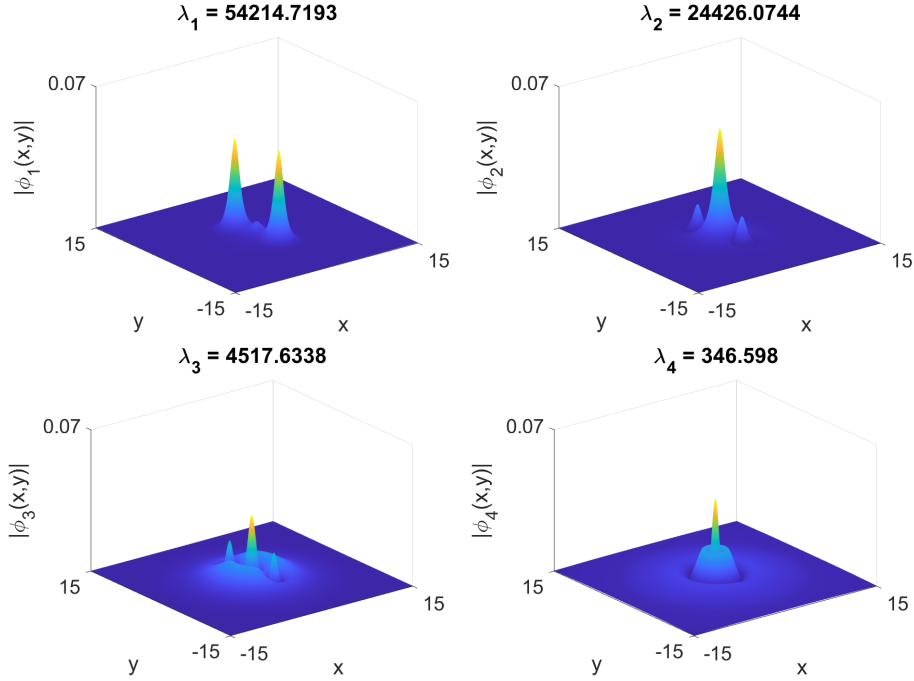


**Figure 2.** The four most dominant modes in the combined soliton evolution data.

Although there is still no analytical solution for this low-dimensional system, i.e., (2.4) where  $n$  is capped at 11, due to its complicated form, simulating just 21 equations instead of the original CQGLE, which typically has over 10,000 ODEs based on how the spatial domain is discretized, is a tremendous improvement in computational efficiency.

**3. Results of the Low-Dimensional Model.** Figure 3 shows the numerical results of our low-dimensional model. As demonstrated in our previous work [13], at a moderate pumping strength of  $g_0 = 1.45$ , the modal amplitudes  $r_n(t)$  and phase differences  $\psi_n(t)$  approach fixed values in the long run. In particular,  $r_2$  (the orange curve in Figure 3) approaches a value of around 1.5 while the other modal amplitudes decay to near zero. This is an important result as it tells us that the shape of  $u(x, y, t)$  should resemble the shape of  $\phi_2$ , a single soliton (see Figure 2), at this  $g_0$  value. The 3-dimensional graph that plots the expansion (2.3) at the steady state, truncated at the 11-th mode, also demonstrates that this low-dimensional model correctly reproduces the qualitative, stable behavior as seen in the full simulation of the CQGLE (see left panel in Figure 1).

At a slightly higher pumping strength around  $g_0 = 2.3$ ,  $r_2$  still remains the most dominant modal amplitude, but the other  $r_n$ 's are more noticeable than before and oscillate periodically over time, as shown in Figure 4. A snapshot of the 3-dimensional view shows that  $u(x, y, t)$  still has the shape of a single soliton. Its width and height, however, undergo persistent fluctuations due to the periodicity in the modal amplitudes.

The time dependence of the modal amplitudes and phase differences disappears when the pumping strength is increased beyond certain critical value. As shown in Figure 5, at a high

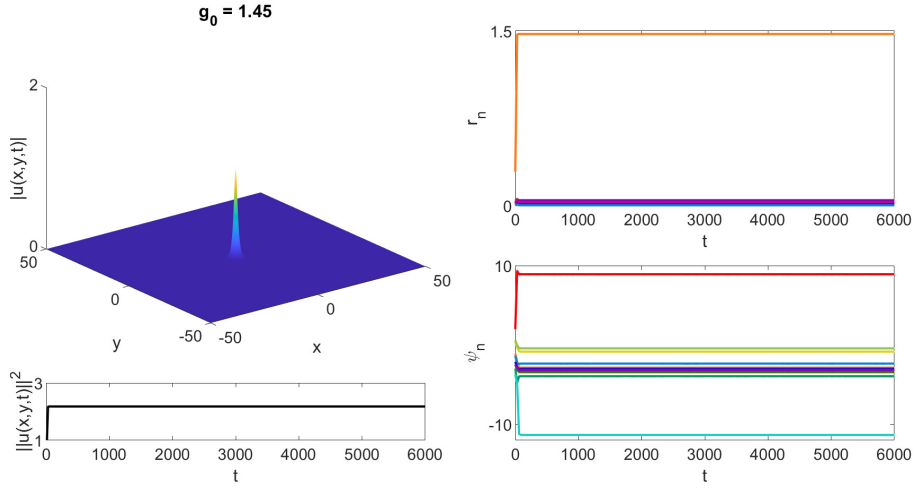


**Figure 3.** Simulation of the low-dimensional model at  $g_0 = 1.45$ . The bottom left panel shows the stable fixed point.

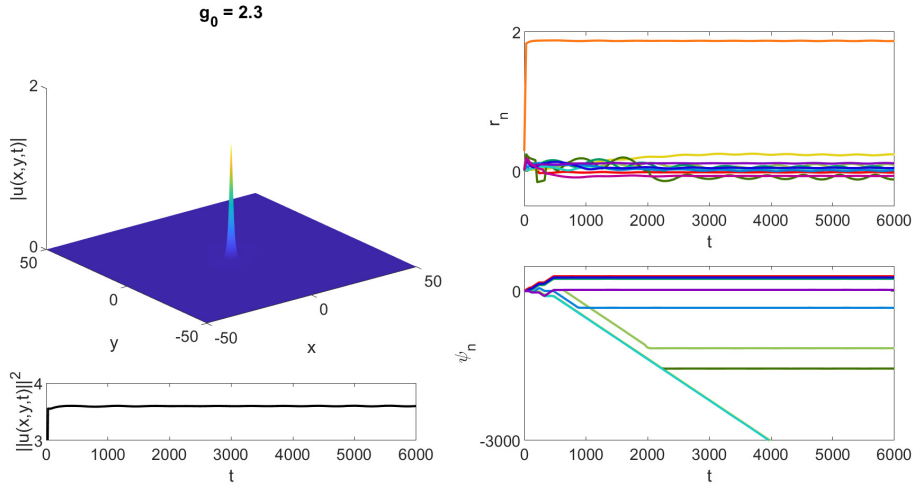


**Figure 4.** Simulation of the low-dimensional model at  $g_0 = 2.3$ .

gain value of  $g_0 = 3.2$ , the modal amplitudes and phase differences stabilize after a brief transient stage. This time, however, it is  $r_7$  (the green curve), a modal amplitude associated primarily with the double-soliton shape, instead of  $r_2$ , that emerges as the dominant modal amplitude at steady state. Contributions from the other  $r_n$ 's are non-negligible and all the modal amplitudes combine to form a clean double pulse, matching the results from the full simulation (see right panel of [Figure 1](#)). At such a high gain, a single-soliton configuration is not sustainable, as the total cavity energy is too high to be contained in one pulse. A double-soliton configuration is a more favorable equilibrium state.

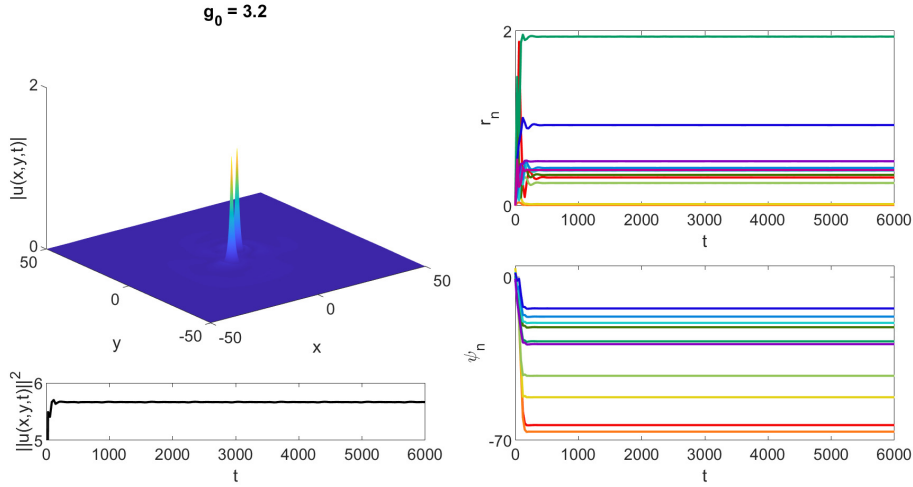


Figure 5. Simulation of the low-dimensional model (2.4) at  $g_0 = 3.2$ .

**4. Linearization.** The ultimate goal of this low-dimensional model was to find its fixed points, which correspond to the different soliton states of the CQGLE. The stability of the single and double solitons can be studied by linearizing the low-dimensional model about these fixed points. Finding fixed points allowed us to mathematically confirm the qualitatively observed long-term behavior of the solitons from the numerical simulations. Specifically, once fixed points were found, their stability could be determined and bifurcations at critical  $g_0$  values could be analyzed using the eigenvalues of the relevant Jacobian matrix.

Fixed points are steady-state values of  $r_n$  and  $\psi_n$  that make the right sides of (2.4) equal to zero, and they can be computed using MATLAB's root-finding algorithm *fsolve*. For this calculation, it is necessary to work with  $\psi_n$  instead of  $\theta_n$ , since the phase angle  $\theta_n$  is constantly changing. Branches of fixed points corresponding to different pumping strengths were computed numerically by means of continuation. Once a solution of the equations  $F_n = 0$  and  $G_n = 0$  at a particular  $g_0$  had been found, it was used as the initial guess of the algorithm to compute the solution at a slightly different  $g_0$  value. Since it is possible that multiple fixed points exist for the same  $g_0$  value, convergence of the root-finding algorithm is highly dependent upon the initial guess used. In practice, it is often easier to use one of the modal amplitudes (e.g.  $r_2$  or  $r_7$ , depending on whether we wanted to find a single-soliton branch or a double-soliton branch) instead of  $g_0$  as the varying parameter. Once the fixed point branches are computed, the Jacobian matrix

$$(4.1) \quad J = \begin{matrix} \begin{bmatrix} \partial F_1 / \partial r_1 & \partial F_1 / \partial r_2 & \dots & \dots & \partial F_1 / \partial \psi_{11} \\ \partial F_2 / \partial r_1 & \partial F_2 / \partial r_2 & \dots & \dots & \partial F_2 / \partial \psi_{11} \\ \vdots & \vdots & \ddots & \ddots & \vdots \\ \partial G_{11} / \partial r_1 & \partial G_{11} / \partial r_2 & \dots & \dots & \partial G_{11} / \partial \psi_{11} \end{bmatrix} \\ (21 \times 21) \end{matrix}$$

at each fixed point is then numerically approximated using central differences. Stability of the fixed point is indicated by the eigenvalues of the Jacobian matrix. Specifically, the fixed point

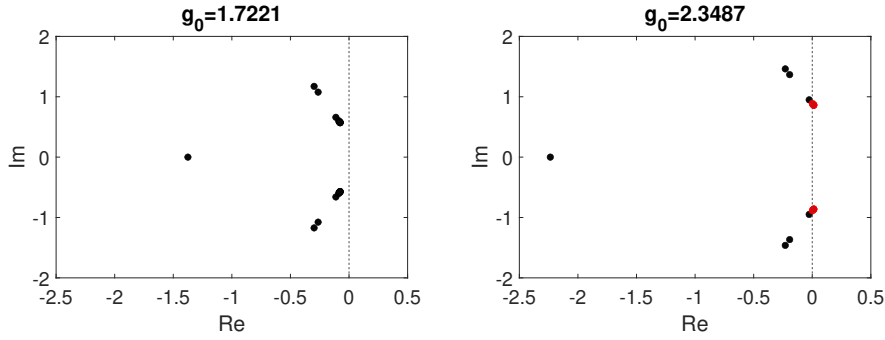


**Figure 6.** Real and imaginary parts of the eigenvalues of the Jacobian matrix at a stable and unstable fixed point. Pairs of eigenvalues cross the imaginary axis as the soliton becomes unstable, which indicate Hopf bifurcations.

is stable if the real parts of all eigenvalues are negative (see left panel of [Figure 6](#)). Otherwise the fixed point is unstable (one example shown in the right panel of [Figure 6](#)).

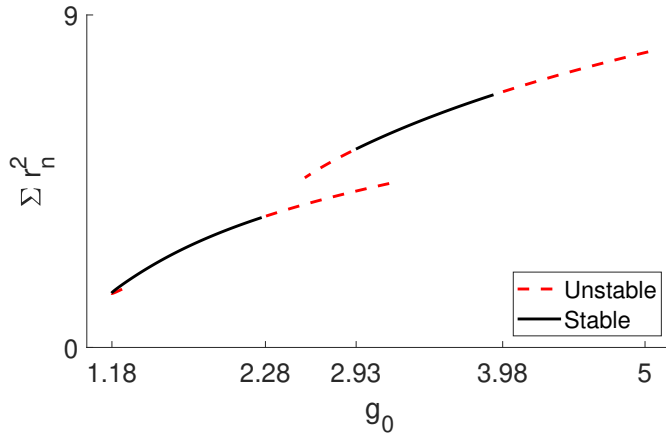


**Figure 7.** Bifurcation diagram showing stability of soliton at different pumping strength values.

[Figure 7](#) plots the bifurcation diagram of the steady-state value of  $\sum r_n^2$  as a function of  $g_0$  based on our low-dimensional model. The branch with smaller amplitudes represents the single solitons while that with greater amplitudes represents the double solitons. A solid curve indicates that the solitons in that range of  $g_0$  values are stable while a dashed curve means that the solitons are unstable. According to the low-dimensional model, solitons will not form for gain values below  $g_0 \approx 1.18$  because pulses are not sustainable at such low pumping strengths. Once  $g_0$  increases above this critical value, a stable branch and an unstable branch of single solitons are formed simultaneously, which suggests that the system undergoes a saddle-node bifurcation at this  $g_0$  value. The single soliton remains stable up to approximately  $g_0 \approx 2.28$  where a pair of complex conjugate eigenvalues cross the imaginary axis from the left half into the right half of the complex plane (see [Figure 6](#) and this [video](#)), which is the signature of a Hopf bifurcation. At this bifurcation value, the single soliton loses stability and a periodic

solution is created, which is exactly what we saw in [Figure 4](#). Another Hopf bifurcation occurs at  $g_0 \approx 2.93$  where the periodic solution is destroyed and the system “jumps” to the stable branch of double solitons. These double solitons eventually lose stability at around  $g_0 \approx 3.98$  through another Hopf bifurcation. After this point, the double-pulse is seen to oscillate periodically over time. We ran full simulations on the CQGLE (1.1) and confirmed that these bifurcations occur at roughly the same  $g_0$  values. The low-dimensional model we built thus qualitatively and efficiently reproduces the essential soliton dynamics governed by the full PDE model.

**5. Conclusions.** We used the singular value decomposition to derive a low-dimensional model that describes the soliton dynamics observed in the complex cubic-quintic Ginzburg-Landau equation. Our low-dimensional model qualitatively reproduced the transition from single to double solitons via an intermediate periodic state as the pumping strength increased. In addition, the bifurcation analysis of the model showed that the creation and destruction of the periodic states were through Hopf bifurcations. Not only was the computational time significantly shortened, the low-dimensional model also gave us a mathematical understanding of the soliton dynamics governed by the CQGLE.

This same process could be used to analyze bifurcations and accompanying changes in soliton behavior due to varying other parameters. For example, soliton behavior notably changes dependent on the sign of the diffraction coefficient  $D$ , so these same methods of dimension reduction and linear stability analysis could be used to mathematically study the case where  $D$  is negative. On a broader scale, the methods demonstrated in this paper could also be applied to other pattern-forming systems.

**Acknowledgments.** The author would like to thank the Department of Mathematics, Physics, and Statistics at Azusa Pacific University (APU) for funding this research through their Mathematics and Physics Fellowship Program, and the Office of Undergraduate Research at APU for their financial support to present this work at several conferences. The author would also like to thank the Society of Women Engineers for accepting and supporting the presentation of this work at their WE22 Conference.

## REFERENCES

- [1] Russell, J.S. (1845). Report on Waves: Made to the Meetings of the British Association in 1842-43.
- [2] Stokes, G.G. (1847). On the Theory of Oscillatory Waves. *Transactions of the Cambridge Philosophical Society*, 8, pp. 441-455.
- [3] Boussinesq, J. (1872). Theorie des ondes et des remous qui se propagent le long d’un canal rectangulaire horizontal, en communiquant au liquide contenu dans ce canal des vitesses sensiblement pareilles de la surface au fond. *Journal de Mathématiques Pures et Appliquées*, 17, pp. 55-108.
- [4] Korteweg, D.G. and de Vries, G. (1895). On the Change of Form of Long Waves Advancing in a Rectangular Canal and a New Type of Long Stationary Waves. *Philosophical Magazine Series*, 39, pp. 422-443.
- [5] Zabusky, N.J. and Kruskal, M.D. (1965). Interaction of “Solitons” in a Collisionless Plasma and the Recurrence of Initial States. *Phys. Rev. Lett.*, 15, pp. 240.
- [6] Osborne, A.R. (2010). Brief History and Overview of Nonlinear Water Waves. *International Geophysics*, 97, pp. 3-31.
- [7] Haus, H.A. (1975). Theory of mode locking with a fast saturable absorber. *J. Appl. Phys.*, 46, pp.

- 3049-3058.
- [8] Ding, E., Luh, K., and Kutz, J. N. (2011). Stability analysis of cavity solitons governed by the cubic-quintic Ginzburg-Landau equation. *Journal of Physics B: Atomic, Molecular and Optical Physics*, 44(065401), pp. 1-7.
  - [9] van Saarloos, W. and Hohenberg, P.C. (1992). Fronts, pulses, sources and sinks in generalized complex Ginzburg-Landau equations. *Physica D: Nonlinear Phenomena*, 56, pp. 303-367.
  - [10] Cross, M.C. and Hohenberg, P.C. (1993). Pattern formation outside of equilibrium. *Rev. Mod. Phys.*, 65, pp. 851.
  - [11] Holmes P., Lumley J.L., and Berkooz, G. *Turbulence, Coherent Structures, Dynamical Systems and Symmetry* (Cambridge University Press, Cambridge, 1996).
  - [12] Ding, E., Shlizerman, E., and Kutz, J. N. (2010). Modeling multipulsing transition in ring cavity lasers with proper orthogonal decomposition. *Physical Review A*, 82(023823), pp. 1-10.
  - [13] Gottry, E. and Ding, E. (2021). Analysis of the 2D complex Ginzburg-Landau Equation using Singular Value Decomposition. *Virginia Journal of Business, Technology, and Science*, 1(1).